Letters in Applied NanoBioScience
Open-Access Journal (ISSN: 2284-6808)

Article
Volume 12, Issue 4, 2023, 180
https://doi.org/10.33263/LIANBS124.180

Citric Acid Mediated Synthesis of Spinel Binary Copper Manganese Oxide ($CuMn_2O_4$) Nanomaterial using Sol-Gel Method

Jagannath S. Godse [1], Sonalika V. Pawar [2], Santosh B. Gaikwad [3], Vishal B. Bhise [4], Sandeep S. Dhotre [5], Sanjay B. Ubale [1,*], Rajendra P. Pawar [5,*]

[1] Department of Chemistry, Deogiri College, Aurangabad - 431 005 (Maharashtra), India
[2] Department of Chemistry, Fergusson College, Pune - 411 004 (Maharashtra), India
[3] Department of Chemistry, L P G Arts and Science College, Shirpur (Jain), Washim – 444 504 (Maharashtra), India
[4] Department of Physics, L P G Arts and Science College, Shirpur (Jain), Washim – 444 504 (Maharashtra), India
[5] Department of Chemistry, Shivchhatrapati College, Aurangabad – 431 005 (Maharashtra), India
* Correspondence: drsanjayubale@gmail.com (S.B.U.), rppawar@yahoo.com (R.P.P.);

Scopus Author ID 7003738785
Received: 1.10.2022; Accepted: 24.11.2022; Published: 25.02.2023

Abstract: This research uses the sol-gel method to investigate a new approach to binary copper manganese oxide ($CuMn_2O_4$) nanomaterial synthesis with citric acid as a surfactant. Water is considered a powerful solvent in this process. The synthetic approach is environmentally beneficial because of its low cost, easy preparation, and industrial feasibility. Analysis of nanomaterial has been done by X-ray diffraction (XRD), transmission electron microscopy (TEM), energy-dispersive X-ray spectroscopy (EDX), and Fourier transform Infrared spectroscopy (FTIR). Highly dispersed characterization results are shown by synthesized nanomaterial. The green procedure proves a practical, eco-friendly, simple, and valuable approach for synthesizing $CuMn_2O_4$ nanomaterial.

Keywords: binary copper manganese oxide; sol-gel method; nanomaterial; citric acid; applications.

1. Introduction

In recent years, nanomaterial has improved massive potential in the research field due to its characteristic properties and large surface-to-volume ratio. It can be used for various applications, such as antimicrobial activities, photovoltaics, sensors, storage devices, drug delivery, and photocatalytic training [1, 2]. Among the various metal oxides, manganese and copper oxide are used due to some practical advantages like readily available, low cost, lesser toxicity, and facile synthesis. In this era, the utilization of binary metal oxide photocatalysts for removing organic pollutants from air and sewerage receives greater attention due to efficient catalytic activity and firmness [3-10].

Spinel structures having the general formula of AB2O4 are renowned materials due to their flexibility in uniting various ions into their crystal structure. The distributions of Cu^{2+} and Mn^{3+} in $CuMn_2O_4$ structure are in tetrahedral and octahedral sites, respectively, which are known as typical

spinel structures; the corresponding general formula is written as AtetB2octO4 [11]. The amounts of Mn4+ species and compositional homogeneity cause the high activity of this spinel compound.

Several methods are available for the preparation of metal oxide nanoparticles. For instance, solid-state synthesis, a hydrothermal method [12-14], an electrochemical, sol-gel technique [15,16], co-precipitation, microwave-assisted synthesis [12,17], Thermal decomposition method [18,19], etc. Due to high temperature and hazardous solvent issues in some of the above methods, we decided to work with the sol-gel method. Among these techniques, the sol-gel method is the greenest and most sophisticated because there is no requirement for high pressure and high temperature, low cost, and the crystalline size and structure of the nanomaterial can be easily monitored by changing the pH of the medium and large amount of sample can be prepared at a time. Hence, in this research article, we have offered the preparation of CuMn2O4 nanoparticles by a simple sol-gel method in the presence of citric acid as a good surfactant.

2. Materials and Methods

2.1. Materials.

Manganese chloride, copper chloride, citric acid, hydrochloric acid, and ammonium hydroxide were purchased from SD-Fine chemical company located in Mumbai (MH), India, and used without further purification. All the aqueous solutions were prepared in distilled water.

2.2. Characterization methods.

The X-ray diffraction (XRD) pattern copper manganese oxide (CuMn2O4) nanomaterial was recorded by the Rigaku X-ray Diffractometer with a Cu K-α radiation source (λ=1.5406 A°) operated at 40 kV. Copper manganese oxide (CuMn2O4) structural morphology was studied using Scanning electron microscopy (SEM) images obtained on Field Emission Scanning Electron Microscope (FESEM) JEOL 6390LA, Japan. Transmission electron microscope (TEM) images and the energy dispersive spectrometry (EDS) analysis were studied by JEOL/JEM 2100, Japan, with an acceleration voltage of 200 kV. Fourier transform infrared (FT-IR) spectra of copper manganese oxide (CuMn2O4) nanomaterial were recorded on the Shimadzu IR spectrophotometer.

2.3. Synthesis of $CuMn_2O_4$ nanoparticles.

Synthesis of $CuMn_2O_4$ spinel oxide nanoparticles was carried out by the sol-gel method. Initially, 0.25 M of Manganese chloride and 0.25 M of copper chloride were dissolved separately in 50 ml of water. 0.1 N hydrochloric acid improves the solubility of Manganese chloride and copper chloride in water. Both solutions were mixed with constant stirring. After mixing the solutions, 1 gm of the citric acid solution was added as a surfactant. The pH of the above solution was adjusted at 8-8.5 (basic) using 3 to 3.5 ml NH_4OH solution. Precipitation was formed, which stirred with constant stirring for an hour at room temperature. The mixture was filtered using Whatman Filter Paper No. 42 and washed with deionized water 2-3 times. The obtained product was dried in an oven at 100˚C for 2 hours. Finally, the dried material was calcinated in the furnace

for 3 hours at 500˚C. The black-colored precipitate was obtained as a final product and was stored for further study.

3. Results and Discussion

3.1. FTIR analysis of $CuMn_2O_4$ oxide nanomaterial.

Fourier transform infrared spectrometer confirms the formation of metal-oxygen (M-O) and metal-metal (MM) bonds in the $CuMn_2O_4$ nanomaterial, as shown in Figure 1. Investigation of nanomaterial is observed at the wavelength range from 397 cm^{-1} to 3980 cm^{-1}. The low-frequency vibrations of the M-O bond appear below 1000 cm^{-1}. In Figure 1, the two firm peaks at positions 686.77 cm^{-1} and 437.84 cm^{-1} represent Cu–O and Mn-O stretching vibrational modes, respectively. These are the primary evidence of $CuMn_2O_4$ formation [20]. The peak at around 823.60 cm^{-1} is detected as the stretching vibration of Cu–Mn and the band that appeared in the range of 1000–1400 cm^{-1} is recognized as the stretching vibration of –OH [21]. The stretching vibrations observed in FTIR spectra are specific to metal oxides in spinel.

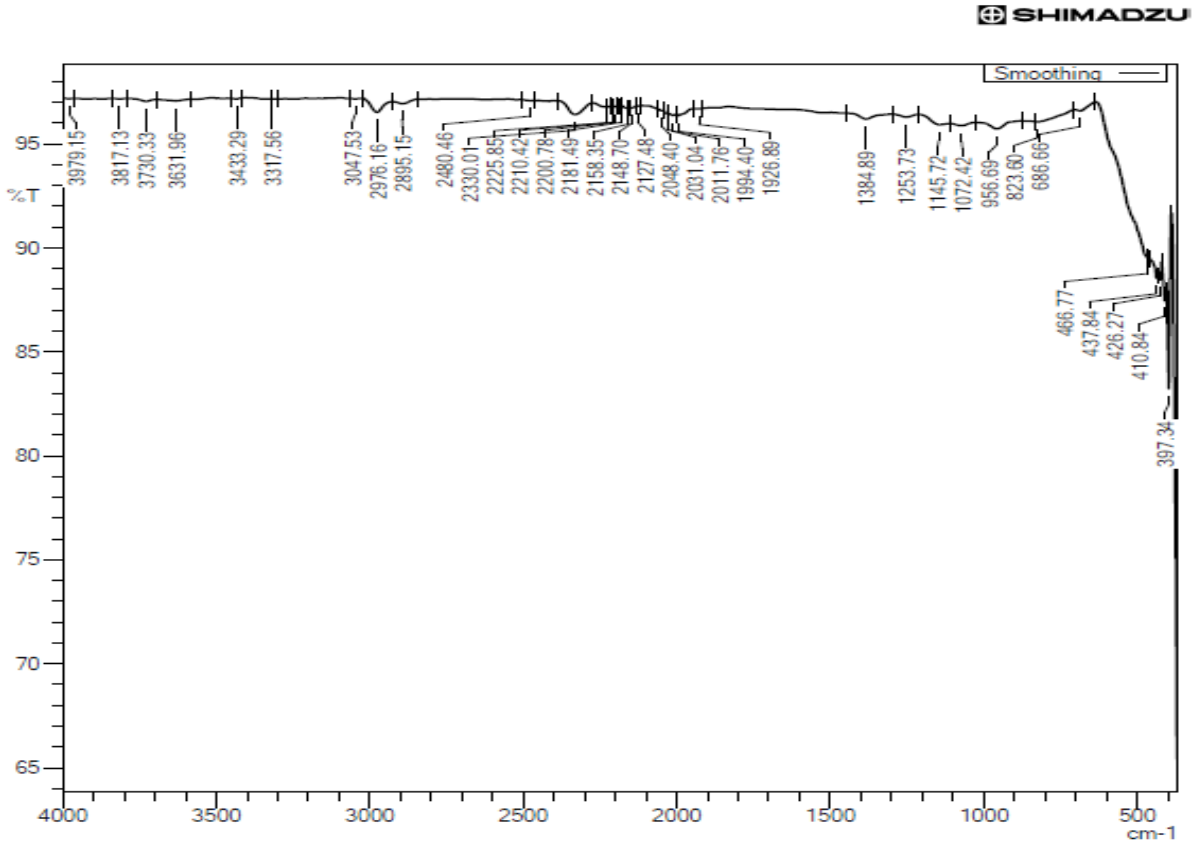

Figure 1. FTIR spectrum of $CuMn_2O_4$ nanoparticles in the spectrum range from 397 cm^{-1} to 3980 cm^{-1}.

3.2. XRD characterization of CuMn2O4 oxide nanomaterial.

The X-ray diffraction technique investigated the chemical, structural, and spectroscopic properties of $CuMn_2O_4$ nanomaterial. All X-ray diffraction peaks were indexed according to the standard data for $CuMn_2O_4$, as shown in Figure 2, which is considered mixed-valent oxides that acquire spinel structures in which the Cu and Mn ions are distributed over tetrahedral (A) and

octahedral (B) sites. The significant peaks are obtained for 2θ at 16.1°,30.48°, 35.64°, 38.72°, 43.66°, 57.82°, and 63.48°, corresponding to the planes (111), (220), (311), (222), (400), (511) and (440) respectively. In addition, the Fd-3m space group and face-centered cubic structure of $CuMn_2O_4$ nanomaterial are recognized in the X-ray diffraction pattern and correctly matched with the standard JCPDS Card No. 01-084-0543 [21, 22]. The average crystallite size (D) of $CuMn_2O_4$ nanomaterial was calculated using the Scherer formula [23].

$$D = K\lambda / \beta Cos\theta$$

where K is a shape factor, D is the size of the nanomaterial, λ is the incident X-ray beam's wavelength, θ is Bragg's diffraction angle, and β is the full-width half maximum. The average particle size of the investigating nanomaterial was 14.47 nm.

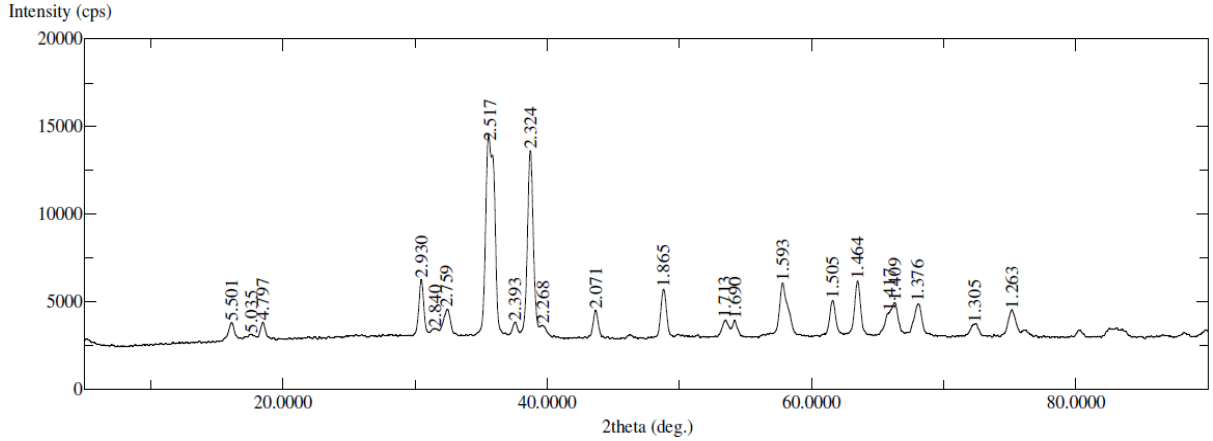

Figure 2. XRD pattern of $CuMn_2O_4$ oxide nanomaterial synthesized by sol-gel technique.

3.3. SEM, TEM & EDX studies of CuMn2O4 oxide nanomaterial.

The morphology and complete structures of $CuMn_2O_4$ nanomaterial were contributed by scanning electron microscope (SEM) and energy-dispersive X-ray (EDX) spectroscopy. SEM images of $CuMn_2O_4$ nanomaterial synthesized by sol-gel method from chloride precursors strengthening the precursors at 500°C are shown in as shown in Figure 3. Scanning Electron Microscope (SEM) instrument in the scale range taken between 500 μm and 1μm.

The elemental compositional investigation of $CuMn_2O_4$nanomaterial is shown in as shown in Figure 4. The presence of Mn and Cu and the Mn/Cu ratio were determined by EDX investigation, which matches perfectly with $CuMn_2O_4$. This confirms the availability of copper, manganese, and oxygen with a weight percentage of 65.73%, 16.9%, and 16.25%, and atomic percentages of 43.3%, 12.88%, and 42.51%, respectively.

Transmission electron microscopy (TEM) images of $CuMn_2O_4$ nanomaterial synthesized showed the $CuMn_2O_4$ nanomaterial has cubical shaped nanomaterial with average particle size between 50.59 nm to 69.83 nm (as shown in Figure 5).

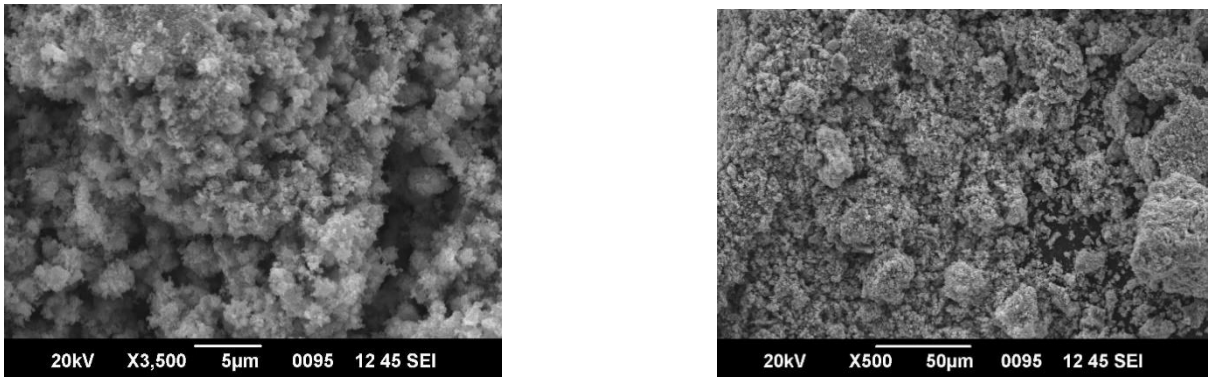

Figure 3. SEM image of copper manganese oxide nanomaterial prepared by sol-gel method.

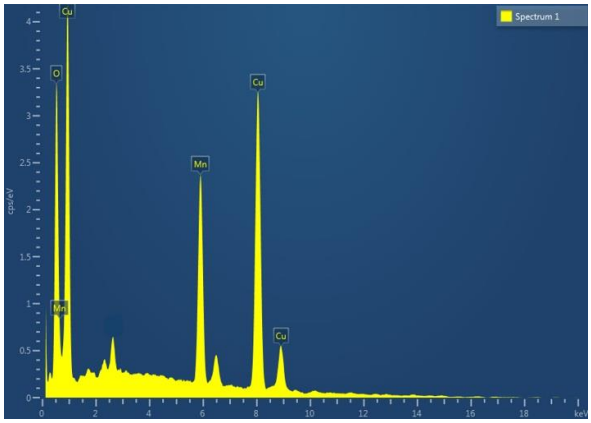

Figure 4. EDX of copper manganese oxide nanomaterial prepared by sol-gel method.

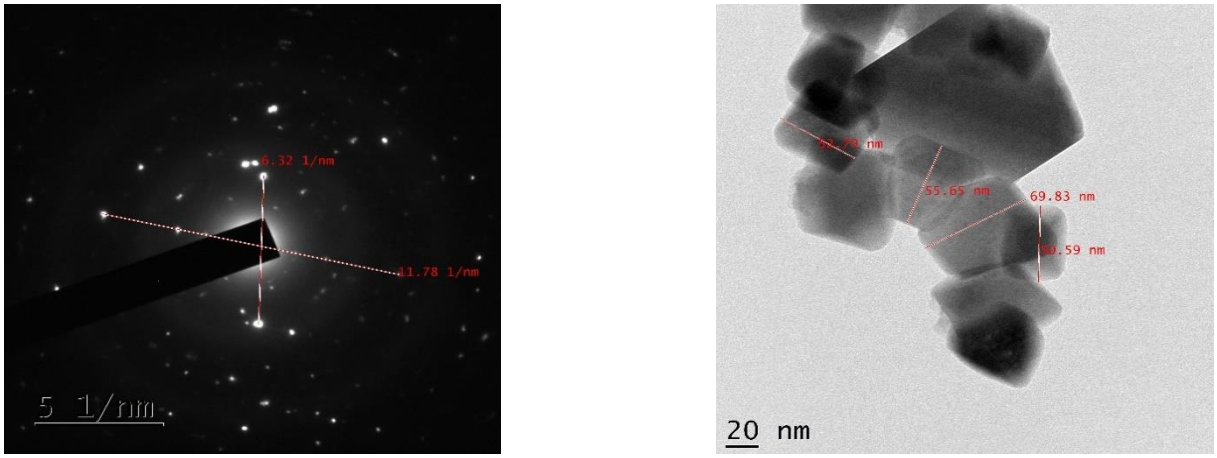

Figure 5. TEM of copper manganese oxide nanomaterial prepared by sol-gel method.

Nanomaterials have had a broader range of applications and use in various fields in recent years. Some researchers have studied the use of nanomaterials for catalytic activity for oxidation [24-26], photocatalytic activity [27-29], a high-performance electrode for supercapacitors [30-33], solid oxide fuel cells [34], amperometric detection of hydrogen peroxide [35] and catalytic ozonation membrane reactor [36-38]. These examples confirm that $CuMn_2O_4$ spinel oxide nanomaterial is environmentally supportive for living organisms and extremely useful in different fields.

4. Conclusions

A cubical-shaped $CuMn_2O_4$ spinel oxide nanomaterial was successfully prepared using a sol-gel, an environmentally supportive method. In synthesizing binary Cu-Mn nanomaterial, copper chloride and manganese chloride bind together using citric acid as a surfactant. This method is eco-friendly, cheap, easy to handle, non-hazardous, and harmless aqueous solvent systems.

Funding

This research received no external funding.

Acknowledgments

This research has no acknowledgment.

Conflicts of Interest

The authors declare no conflict of interest.

References

1. Vaseem, M.; Umar, A.; Hahn, Y.B.; Kim, D.H.; Lee, K.S.; Jang, J.S.; Lee, J.S. Flower shaped CuO nanostructures: structural, photocatalytic and XANES studies. *Catal. Commun*. **2008,** *10*, 11–16, https://doi.org/10.1016/j.catcom.2008.07.022.
2. Arulraj, A.; Govindan, S.; Vadivel, S.; Subramanian, B. Photovoltaic performance of TiO_2 using natural sensitizer extracted from Phyllanthus Reticulatus, Journal of Material Science: *Materials in Electronics* **2017**, *28*, 18455-18462, https://doi.org/10.1007/s10854-017-7792-7.
3. Zuo, G.M.; Cheng, Z.X.; Chen, H.; Li, G.W.; Miao, T. Study on photocatalytic degradation of several volatile organic compounds, *J. Hazard. Mater.* B **2006,** *128*, 158-163, https://doi.org/10.1016/j.jhazmat.2005.07.056.
4. Magdalane, C. M.; Kaviyarasu, K.; Vijaya, J. J.; Siddhardha, B.; Jeyaraj, B.; Kennedy, J.; Maaza, M. Evaluation on the heterostructured CeO_2/Y_2O_3 binary metal oxide nanocomposites for UV/Vis light induced photocatalytic degradation of Rhodamine-B dye for textile engineering application. *Journal of Alloys and Compounds* **2017**, *727*, 1324-1337, https://doi.org/10.1016/j.jallcom.2017.08.209.
5. Anpo, M.; Ichihashi, Y.; Takeuchi, M.; Yamashita, H. Design of unique titanium oxide photocatalysts by an advanced metal ion-implantation method and photocatalytic reactions under visible light irradiation. *Res. Chem. Intermed.* **1998**, *24*, 143-149, https://doi.org/10.1163/156856798X00735.
6. Kasinathan, K.; Kennedy, J.; Elayaperumal, M.; Henini, M.; Malik, M. Photodegradation of organic pollutants RhB dye using UV simulated sunlight on ceria based TiO_2 nano materials for antibacterial applications. *Scientific reports* **2016**, *6*, 38064, https://doi.org/10.1038/srep38064.
7. Anpo, M.; Ichihashi, Y.; Takeuchi, M.; Yamashita, H. Design and development of unique titanium oxide photocatalysts capable of operating under visible light irradiation by an advanced metal ion-implantation method. *Stud. Surf. Sci. Catal.* **1999**, *121*, 305-310, https://doi.org/10.1016/S0167-2991(99)80084-6.
8. Magdalane, C. M.; Kaviyarasu, K.; Vijaya, J. J.; Siddhardha, B.; Jeyaraj, B. Facile synthesis of heterostructured cerium oxide/yttrium oxide nanocomposite in UV light induced photocatalytic degradation and catalytic reduction: synergistic effect of antimicrobial studies. *Journal of Photochemistry and Photobiology B: Biology* **2017**, *173*, 23-34, https://doi.org/10.1016/j.jphotobiol.2017.05.024.
9. Anpo, M.; Che, M. Applications of photoluminescence techniques to the characterization of solid surfaces in relation to adsorption, catalysis, and photocatalysis. *Adv. Catal.* **1999**, *44*, 119-257, https://doi.org/10.1016/S0360-0564(08)60513-1.
10. Kudo, A.; Sekizawa, M. Photocatalytic H_2 evolution under visible light irradiation on Ni-doped ZnS photocatalysts. *Chem. Commun*. **2000**, 1371-1372, https://doi.org/10.1039/B003297M.

11. Tang, Z.R.; Kondrat, S.A.; Dickinson, C.; Bartley, J.K.; Carley, A.F.; Taylor, S.H.; Davies, T.E.; Allix, M.; Rosseinsky, M.J.; Claridge, J.B.; Xu, Z.; Romani, S.; Crudace, M.J.; Hutchings, G.J. Synthesis of high surface area $CuMn_2O_4$ by supercritical anti-solvent precipitation for the oxidation of CO at ambient temperature. *Catal. Sci. Technol*. **2011**, *1*, 740-746, https://doi.org/10.1039/C1CY00064K.
12. Sumithra, T.; Pearline, C. L.; Abel, M. J.; Pramothkumar, A.; Inbaraj, P. F. H.; Prince, J. J. Studies on structural and optical behavior of $SnO_2/CuMn_2O_4$ nanocomposite developed via two-step approach for photocatalytic activity. *Materials Research Express* **2019,** *6*, 115047, https://iopscience.iop.org/article/10.1088/2053-1591/ab45a3.
13. Salavati-Niasari, M.; Davar, F.; Loghman-Estarki, M. R. Long chain polymer assisted synthesis of flower-like cadmium sulfide nanorods via hydrothermal process. *Journal of Alloys and Compounds* **2009,** *481*, 776-780, https://doi.org/10.1016/j.jallcom.2009.03.086.
14. Hamed, S.; Hossein, K.; Masoud, S.-N.; Sobhan, M.-D. Enhanced photocatalytic degradation of dyes over graphene/Pd/TiO_2 nanocomposites: TiO_2 nanowires versus TiO_2 nanoparticles. *Journal of Colloid and Interface Science* **2017,** *498*, 423-432, https://doi.org/10.1016/j.jcis.2017.03.078.
15. Maryam, M.; Faezeh, S.; Fatemeh, A.; Masoud, S.-N. Grafting of $CuFe_{12}O_{19}$ nanoparticles on CNT and graphene: Eco-friendly synthesis, characterization and photocatalytic activity. *Journal of Cleaner Production* **2018,** *176*, 1185-1197, https://doi.org/10.1016/j.jclepro.2017.11.177.
16. Salavati-Niasari, M.; Farhadi-Khouzani, M.; Davar, F. J. Bright blue pigment $CoAl_2O_4$ nanocrystals prepared by modified sol–gel method. *Journal of Sol-Gel Science and Technology* **2009,** *52*, 321-327, https://doi.org/10.1007/s10971-009-2050-y.
17. Mir, N.; Salavati-Niasari, M.; Davar, F. Preparation of ZnO nanoflowers and Zn glycerolate nanoplates using inorganic precursors via a convenient rout and application in dye sensitized solar cells. *Chemical Engineering Journal* **2012,** *181*, 779-789, https://doi.org/10.1016/j.cej.2011.11.085.
18. Goudarzi, M.; Mir, N.; Mousavi-Kamazani, M.; Bagheri, S.; Salavati-Niasari, M. Biosynthesis and characterization of silver nanoparticles prepared from two novel natural precursors by facile thermal decomposition methods. *Scientific Reports* **2016,** *6*, 1-13, https://doi.org/10.1038/srep32539.
19. Davar, F.; Salavati-Niasari, M.; Mir, N.; Saberyan, K.; Monemzadeh, M.; Ahmadi, E. Thermal decomposition route for synthesis of Mn_3O_4 nanoparticles in presence of a novel precursor. *Polyhedron* **2010,** *29*, 1747-1753, https://doi.org/10.1016/j.poly.2010.02.026.
20. Mungse, P.; Saravanan, G.; Uchiyama, T.; Nishibori, M.; Teraoka, Y.; Rayalu, S.; Labhsetwar, N. Copper–manganese mixed oxides: CO 2-selectivity, stable, and cyclic performance for chemical looping combustion of methane. *Phys. Chem. Chem. Phys*. **2014,** *16*, 19634-19642, https://doi.org/10.1039/C4CP01747A.
21. Pramothkumar, A.; Senthilkumar, N.; Jothivenkatachalam, K. J. Flake-like $CuMn_2O_4$ nanoparticles synthesized via co-precipitation method for photocatalytic activity. *Physica B: Condensed Matter* **2019,** *572*, 117-124, https://doi.org/10.1016/j.physb.2019.07.047.
22. Saravanakumar, B.; Lakshmi, S. M.; Ravi, G.; Ganesh, V.; Sakunthala, A.; Yuvakkumar, R. Electrochemical properties of rice-like copper manganese oxide ($CuMn_2O_4$) nanoparticles for pseudocapacitor applications. *Journal of Alloys and Compounds* **2017,** *723*, 115-122, https://doi.org/10.1016/j.jallcom.2017.06.249.
23. Enhessari, M.; Salehabadi, A.; Maarofian, K.; Khanahmadzadeh, S. Synthesis and physicochemical properties of $CuMn_2O_4$ nanoparticles; a potential semiconductor for photoelectric devices. *International Journal of Bio-Inorganic Hybrid Nanomaterials* **2016,** *5*, 115-120.
24. Solt, H. E.; Németh, P. t.; Mohai, M. s.; Sajó, I. n. E.; Klébert, S.; Franguelli, F. P.; Fogaca, L. A.; Pawar, R. P.; Kótai, L. Temperature-limited synthesis of copper manganites along the borderline of the amorphous/crystalline state and their catalytic activity in CO oxidation. *ACS Omega* **2021,** *6*, 1523-1533, https://doi.org/10.1021/acsomega.0c05301.
25. Zhang, Y.; Li, Y.; Zeng, Z.; Hu, J.; Hou, Y.; Huang, Z. Synergically engineering Cu^+ and oxygen vacancies in $CuMn_2O_4$ catalysts for enhanced toluene oxidation performance. *Molecular Catalysis* **2022,** *517*, 112043, https://doi.org/10.1016/j.mcat.2021.112043.
26. Wan, X.; Tang, N.; Xie, Q.; Zhao, S.; Zhou, C.; Dai, Y.; Yang, Y. A $CuMn_2O_4$ spinel oxide as a superior catalyst for the aerobic oxidation of 5-hydroxymethylfurfural toward 2, 5-furandicarboxylic acid in aqueous solvent. *Catal. Sci. Technol.* **2021,** *11*, 1497-1509, https://doi.org/10.1039/D0CY01649G.

27. Sobhani, A. Hydrothermal synthesis of $CuMn_2O_4$/CuO nanocomposite without capping agent and study its photocatalytic activity for elimination of dye pollution. *International Journal of Hydrogen Energy* **2022**, *47*, 20138-20152, https://doi.org/10.1016/j.ijhydene.2022.04.149.
28. Albukhari, S. M.; Alsheheri, S. Z.; Mahmoud, M.; Ismail, A. A. Construction of mesoporous $CuMn_2O_4$/g-C_3N_4 heterojunctions as effective photocatalysts for reduction and removal of mercury ions. *Journal of Materials Science: Materials in Electronics* **2022,** *33*, 190-202, https://link.springer.com/article/10.1007/s10854-021-07284-5.
29. Abirami, R.; Senthil, T.; Kalaiselvi, C. R. Preparation of pure $PbTiO_3$ and (Ag–Fe) codoped $PbTiO_3$ perovskite nanoparticles and their enhanced photocatalytic activity. *Solid State Communications* **2021,** *327*, 114232, https://doi.org/10.1016/j.ssc.2021.114232.
30. Zhang, C.; Xie, A.; Zhang, W.; Chang, J.; Liu, C.; Gu, L.; Duo, X.; Pan, F.; Luo, S. $CuMn_2O_4$ spinel anchored on graphene nanosheets as a novel electrode material for supercapacitor.*Journal of Energy Storage* **2021,** *34*, 102181, https://doi.org/10.1016/j.est.2020.102181.
31. Cheng, C.; Cheng, Y.; Lai, G. $CuMn_2O_4$ hierarchical microspheres as remarkable electrode of supercapacitors. *Materials Letters* **2022,** *317*, 132102, https://doi.org/10.1016/j.matlet.2022.132102.
32. Aouini, S.; Bardaoui, A.; Santos, D. M.; Chtourou, R. Hydrothermal synthesis of $CuMn_2O_4$ spinel-coated stainless steel mesh as a supercapacitor electrode. Journal of Materials Science: *Materials in Electronics* **2022**, 1-8, https://doi.org/10.1007/s10854-022-08219-4.
33. Sheikhzadeh, M.; Sanjabi, S. Coelectrodeposition of crystalline copper-manganese oxide containing $CuMn_2O_4$ spinel for high energy supercapacitor application. *Synthetic Metals* **2021,** *278*, 116802. https://doi.org/10.1016/j.synthmet.2021.116802
34. Acharya, N.; Chaitra, U.; Vijeth, H.; Sagar, R. Highly dense Mn_3O_4 and $CuMn_2O_4$ spinels as efficient protective coatings on solid oxide fuel cell interconnect and their chromium diffusion studies. *Journal of Alloys and Compounds* **2022**, *918*, 165377, https://doi.org/10.1016/j.jallcom.2022.165377.
35. Gao, Y.; Li, B.; Zhang, Z.; Zhang, X.; Deng, Z.; Huo, L.; Gao, S. $CuMn_2O_4$ spinel nanoflakes for amperometric detection of hydrogen peroxide. *ACS Appl. Nano Mater.* **2021,** *4*, 6832-6843, https://doi.org/10.1021/acsanm.1c00898.
36. Liu, Y.; Song, Z.; Wang, W.; Wang, Z.; Zhang, Y.; Liu, C.; Wang, Y.; Li, A.; Xu, B.; Qi, F. A $CuMn_2O_4$/g-C_3N_4 catalytic ozonation membrane reactor used for water purification: Membrane fabrication and performance evaluation. *Separation and Purification Technology* **2021,** *265*, 118268, https://doi.org/10.1016/j.seppur.2020.118268.
37. Li, A.; Liu, Y.; Wang, Z.; Song, Z.; Zhang, Y.; Wang, Y.; Xu, B.; Qi, F.; Ikhlaq, A.; Kumirska, J.; Siedlecka, E.M. Catalytic ozonation membrane reactor integrated with $CuMn_2O_4$/rGO for degradation emerging UV absorbers (BP-4) and fouling in-situ self-cleaning. *Separation and Purification Technology* **2021,** *279*, 119804, https://doi.org/10.1016/j.seppur.2021.119804.
38. Ikhlaq, A.; Zafar, M.; Javed, F.; Yasar, A.; Akram, A.; Shabbir, S.; Qi, F. Catalytic ozonation for the removal of reactive black 5 (RB-5) dye using zeolites modified with $CuMn_2O_4$/gC_3N_4 in a synergic electro flocculation-catalytic ozonation process. *Water Sci. Technol*. **2021,** *84*, 1943-1953, https://doi.org/10.2166/wst.2021.404.